Anal. Chem. **1997,** *69,* 1931−1935

Comparison of Phase Rotation, Phase Spectrum, and Two-Dimensional Correlation Methods in Step-Scan Fourier Transform Infrared Photoacoustic Spectral Depth Profiling

Eric Y. Jiang† and Richard A. Palmer*

Department of Chemistry, Duke University, Durham, North Carolina 27708

This paper compares three photoacoustic phase-related analytical approaches for spectral depth profiling of heterogeneous materials, particularly in conjunction with step-scan Fourier transform infrared spectroscopy. The three approaches compared are (1) the phase rotation method, (2) the direct analysis of the phase spectrum, and (3) the calculation of two-dimensional (2D) frequency correlation maps. The experimental data for a representative two-layer sample consisting of a 12-μm-thick layer of ethylene−vinyl acetate on a 60-μm-thick polypropylene substrate are compared for the three approaches. Similar/identical phase difference information can be obtained from either the continuous phase rotation plot or the phase spectrum. However, the phase spectrum method provides more accurate, direct, and efficient results with a higher depth resolution than does the phase rotation method. Qualitative agreement between the 2D correlation analysis and the photoacoustic phase analysis is observed, although the 2D approach does not clearly distinguish between spectral bands with similar response phase, limiting it to qualitative use.

Although the photothermal effect [most often used in the sample−gas−microphone photoacoustic spectroscopy (PAS) technique] can be used for nondestructive spectral depth profiling in any region of the electromagnetic spectrum, it is particularly effective in the infrared. Especially for organic materials, distinctive infrared functional group absorption bands afford layer and/or component identification that is not often possible in the UV/visible region. In the infrared, the broad spectral range and high throughput of Fourier transform interferometry (FT-IR) make it the most versatile spectral technique for use with photoacoustic (PA) detection, and because of the importance of the phase dependence of the PA signal, the step-scan (S^2) mode of FT-IR is the technique of choice for infrared PA spectral depth profiling.

The use of S^2FT-IR PAS for spectral depth profiling has been developed during the past 8 years.[1−11] Since the step-scan mode allows the interferogram to be measured point-by-point, while the optical path difference is held constant, the time dependence of the interferogram is eliminated. This allows a single modulation frequency to be applied to all wavelengths, in contrast to the wavelength-dependent Fourier frequencies of the conventional continuous-scan FT-IR method. This then leads to two important advantages of S^2FT-IR for PA detection: (1) constant thermal sampling depth μ as a function of wavelength [$\mu = (\alpha/\pi f)^{1/2}$, where α is the thermal diffusivity and f is the single modulation frequency] and (2) the ability to easily extract the relative PA signal *phase*, free of instrumental distortion, by use of a lock-in amplifier[4] or digital signal processor.[12−14] (These advantages can also be extended to modulation and demodulation at more than one discrete frequency.) The phase (θ) and magnitude (M) spectra can be obtained from the simultaneous recording of the in-phase (I) and quadrature (Q) spectral components of the signal, according to eqs 1 and 2. In the calculation of the PA signal phase

$$\theta(\sigma) = \tan^{-1}[Q(\sigma)/I(\sigma)] \quad (1)$$

$$M(\sigma) = [Q(\sigma)^2 + I(\sigma)^2]^{1/2} \quad (2)$$

$\theta(\sigma)$, the wavelength-dependent instrument phase cancels out.[15]

There are two basic approaches to PA spectral depth profiling: (1) variation of the modulation frequency and (2) analysis of the signal phase. Application of the modulation frequency variation method (by use of path difference, or phase, modulation) in S^2FT-IR PA depth profiling of both continuously heterogeneous and discretely heterogeneous materials has been widely

† Current address: Bio-Rad Laboratories, Inc., Digilab Division, Cambridge, MA 02139.

(1) Manning, C. J.; Widder, J. M.; Palmer, R. A.; Chao, J. L. *Proc. SPIE-Int. Soc. Opt. Eng.* **1989**, *1145*, 575.
(2) Michaelian, K. H. *Appl. Spectrosc.* **1989**, *43*, 185.
(3) Michaelian, K. H. *Appl. Spectrosc.* **1991**, *45*, 302.
(4) Dittmar, R. M.; Chao, J. L.; Palmer, R. A. *Appl. Spectrosc.* **1991**, *45*, 1104.
(5) Palmer, R. A.; Dittmar, R. M. *Thin Solid Films, Sect. A* **1993**, *223*, 31.
(6) Palmer, R. A.; Jiang, E. Y.; Chao, J. L. *Proc. SPIE-Int. Soc. Opt. Eng.* **1993**, *2089*, 250.
(7) Dittmar, R. M.; Palmer, R. A.; Carter, R. O., III. *Appl. Spectrosc. Rev.* **1994**, *29*, 171.
(8) Jiang, E. Y.; Palmer, R. A.; Chao, J. L. *Abstracts of the Pittsburgh Conference on Analytical Chemistry and Applied Spectroscopy*, Chicago, IL, Feb 27−March 4, 1994; Paper 512P.
(9) McClelland, J. F.; Jones, R. W.; Luo, S. *Abstracts of the Pittsburgh Conference on Analytical Chemistry and Applied Spectroscopy*, Atlanta, GA, March 8−12, 1993; Paper 181.
(10) McClelland, J. F.; Jones, R. W.; Ochiai, S. *Proc. SPIE-Int. Soc. Opt. Eng.* **1993**, *2089*, 302.
(11) Palmer, R. A.; Jiang, E. Y. *J. Phys. IV* **1994**, *4* (July), C7−337.
(12) Manning, C. J.; Griffiths, P. R. *Appl. Spectrosc.* **1993**, *47*, 1345.
(13) Jiang, E. Y.; Powell, J. R.; Curbelo, R.; Barber, L. L.; Crocombe, R. A.; Drapcho, D. L. *Abstracts of the Pittsburgh Conference on Analytical Chemistry and Applied Spectroscopy*, Chicago, IL, March 3−8, 1996; Paper 430.
(14) Drapcho, D. L.; Curbelo, R.; Jiang, E. Y.; Crocombe, R. A.; McCarthy, W. J. *Appl. Spectrosc.* In press.
(15) Manning, C. J.; Dittmar, R. M.; Chao, J. L.; Palmer, R. A. *Infrared Phys.* **1992**, *33*, 53.

S0003-2700(96)01080-3 CCC: $14.00

demonstrated.[1−5,16] However, with this method, the depth resolution is limited by the phase modulation frequency range and frequency selection of the instrument. Furthermore, with sine wave phase modulation, each frequency requires a separate scan. Square wave modulation offers the prospect of demodulation at several odd harmonics as well as the fundamental,[13,14] but in either case only qualitative estimates of relative depth can be made from comparison of the data taken at different frequencies.

The use of the phase of the PA signal, either alone or in combination with variation of the modulation frequency, offers the prospect of much greater detail in depth profiling than use of the modulation frequency alone.[6,17] In addition, theoretical modeling of the phase offers more promise of success.[18−20] The use of the PA phase for depth profiling has been approached in three fairly distinct ways: In the first approach, rotation of the detection phase either in a trial-and-error approach[4,5,7] or by systematic, continuous rotation[8,9,11] has been used to eliminate certain bands from the spectrum or to illustrate the variation of intensity of all bands as a function of detection phase. This method has been used for numerous qualitative studies.[4,5,7−9] In addition, by comparing the "extinction" angles of selected bands, quantitative results can be obtained.[10,11]

The second way of using the phase data is to calculate the phase spectrum $\theta(\sigma)$ (eq 1). The same difference in phase angle obtained from the comparison of extinction angles can also be obtained more directly and with less manipulation from the phase spectrum. While both the phase rotation and phase spectrum methods produce *relative* phase data, the phase can be approximately calibrated in either case by use of a saturated (strongly absorbing) material such as carbon black to establish a "surface phase" reference. The use of either method for measurement of the *absolute* PA phase is limited by the ability to reproduce the *instrument phase* from reference to sample. Nevertheless, the *differences* between the phases of signals for different bands in a spectrum are highly reproducible (±0.3°). For this reason, the phase difference $\Delta\theta$ has been made the focus of a conceptually simple, general theoretical model, which is particularly applicable to discretely laminar materials with distinctive marker bands for each layer.[18,19] To interpret the phase data from materials with continuous variation of composition and only overlapping absorption bands, more sophisticated models have also been proposed.[20]

The third way to use PA phase data is in the calculation of two-dimensional (2D) frequency correlation maps.[21−23] This method was initially used to analyze the responses of polymer films to mechanical strain[24] and the response of liquid crystals to electric fields.[25] Its application to PA depth profiling is a straightforward extension of this work. The synchronous and asynchronous correlation maps provide qualitative insight into the relative depths of layers and/or components.

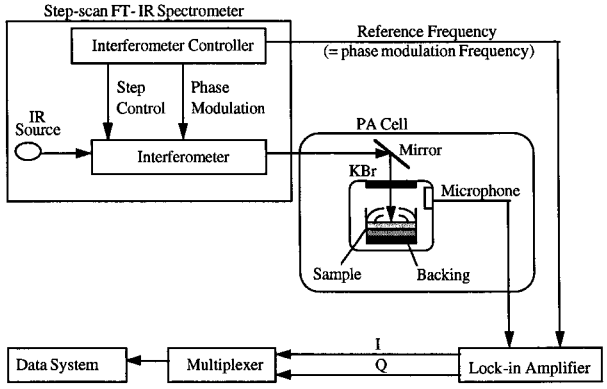

Figure 1. Experimental setup for S²FT-IR PAS depth profiling. Two orthogonal spectral components (*I* and *Q*) are collected from a dual channel LIA referenced to the phase modulation frequency.

It is useful to note that the same initial "raw" data are used in each of the above approaches, i.e., the two orthogonal components of the PA signal, $I(\sigma)$ and $Q(\sigma)$ (ideally, referenced to a spectrum of a standard sample). From these data, the magnitude $M(\sigma)$ and phase $\theta(\sigma)$ spectra can be calculated (eqs 1 and 2). The amplitude of the in-phase signal as a function of detection phase can then be calculated by simple vector rotation,

$$e^{i\alpha}M(\sigma)e^{i\theta} = M(\sigma)e^{i(\alpha+\theta)} = M(\sigma)\cos(\alpha+\theta) + iM(\sigma)\sin(\alpha+\theta) \quad (3)$$

or the phase spectrum $\theta(\sigma)$ can be used directly and $\Delta\theta$ measured, or the 2D synchronous $\Phi(\sigma_1,\sigma_2)$ and asynchronous $\Psi(\sigma_1,\sigma_2)$ correlation spectra (maps) can be calculated according to Noda's definition,[24]

$$\Phi(\sigma_1,\sigma_2) = (^1/_2)M(\sigma_1)M(\sigma_2)\cos[\theta(\sigma_1) - \theta(\sigma_2)] \quad (4)$$

$$\Psi(\sigma_1,\sigma_2) = (^1/_2)M(\sigma_1)M(\sigma_2)\sin[\theta(\sigma_1) - \theta(\sigma_2)] \quad (5)$$

EXPERIMENTAL SECTION

As shown in Figure 1, the experimental setup for collecting the data presented in this paper included a Duke/IBM IR44 FT-IR spectrometer with optional step-scan operation, an MTEC 100 PA detector, and an EG&G PARC 5210 lock-in amplifier (LIA).[5] The spectrometer was purged with CO_2-free dry air produced by a Balston air dryer. Helium gas was chosen to purge the PA cell because of its superior thermoacoustic coupling properties. The PA signal was generated by sinusoidal dither of the moving mirror (phase modulation). The two orthogonal demodulated outputs, *I* and *Q*, were sent first to the multiplexer and then to an eight-bit analog-to-digital converter (ADC) for data processing.

A cylindrical piece of 60% carbon black-filled elastomer was used as both the instrument optical throughput reference and the surface phase reference sample. A two-layer sample of 12-μm ethylene−vinyl acetate copolymer on a 60-μm polypropylene substrate (EVAc/PP) was prepared by casting DuPont Elvax vinyl resin (grade 360) from a benzene solution onto a PP sheet.

A modulation frequency of 200 Hz is chosen in the experiment so as to effectively detect PAS signals from both layers of the sample. Under this condition, the thermal diffusion depths for

(16) McClelland, J. F.; Jones, R. W.; Luo, S.; Seaverson, L. M. A Practical Guide to FTIR Photoacoustic Spectroscopy. In *Practical Sampling Techniques for Infrared Analysis*; Coleman, P., Ed.; CRC Press: Boca Raton, FL, 1993.
(17) Mongeau, B.; Rousset, G.; Bertrand, L. *Can. J. Phys.* **1986**, *64*, 1056.
(18) Jiang, E. Y.; Palmer, R. A.; Connors, L. M.; Chao, J. L. *Abstracts of the Pittsburgh Conference on Analytical Chemistry and Applied Spectroscopy*, New Orleans, LA, March 6−9, 1995; Paper 1044.
(19) Jiang, E. Y.; Palmer, R. A.; Chao, J. L. *J. Appl. Phys.* **1995**, *78*, 460.
(20) Power, J. F.; Prystay, M. C. *Appl. Spectrosc.* **1995**, *49*, 725.
(21) Story, G. M.; Marcott, C.; Noda, I. *Proc. SPIE-Int. Soc. Opt. Eng.* **1993**, *2089*, 242.
(22) Marcott, C.; Story, G. M.; Noda, I. *Abstracts of the Pittsburgh Conference on Analytical Chemistry and Applied Spectroscopy*, New Orleans, LA, March 6−9, 1995; Paper 1043.
(23) Jiang, E. Y. Ph.D. Dissertation, Duke University, Durham, NC, 1995.
(24) Noda, I. *Appl. Spectrosc.* **1990**, *44*, 550.
(25) Nakano, T.; Yokoyama, T.; Toriumi, H. *Appl. Spectrosc.* **1993**, *47*, 1354.

Table 1. PAS Magnitude (M), Phase (θ),[4] and Phase Shift ($\Delta\theta$) Data of EVAc (12 μm) on PP (60 μm) Collected at a Modulation Frequency of 200 Hz

peak (cm^{-1})	vibrational mode assignment	absorbing layer(s)	M	θ (deg)	$\Delta\theta_r$ (deg)	$\Delta\theta_s$ (deg)
A_1 (1740)	C═O stretching	EVAc	1.16	19.4	3	2.9
A_2 (1243)	C—O stretching	EVAc	1.12	20.4	3	4.9
B (1169)	C—C stretching	PP	0.26	53.3	38	36.8
C_1 (2922)	C—H stretching	EVAc/PP	1.24	16.5	0	0.0
C_2 (1378)	C—H bending	EVAc/PP	0.81	36.4	20	19.9
C_3 (1463)	C—H bending	EVAc/PP	0.77	38.6	20	22.1

[a] The PAS phase shift of each band from band C_1 was obtained from the phase rotation $\Delta\theta_r$ and phase spectrum $\Delta\theta_s$ methods, respectively. Note that bands of the same layer may have different PAS phase responses due to the absorptivity (roughly proportional to the PAS peak height or magnitude value) differences. Since the selected bands A_1 and A_2 of the EVAc layer have very similar optical absorptivities, their PAS phases are very close. Readers who are interested in this issue may refer to a previous publication,[19] in which the effect of absorptivity on PAS phase in a multilayer sample system is quantitatively elucidated.

homogeneous pure EVAc and PP are 14.6 and 11.1 μm, respectively. In the layered EVAc/PP sample studied in this paper, however, the effective detection depth of the PP layer can be much greater than that in the homogeneous case (signals as deep as about twice the thermal diffusion depth of EVAc are still detectable), because the EVAc layer is transparent at the energy of a distinctive PP band.[5]

LabCalc-compatible array basic programs *phmag.ab* and *phrot.ab* (developed in-house) were used to calculate phase, magnitude, and rotated spectra. 2D-IR PAS correlation maps were created by using the Galactic Industries *2D-IR.ab* program and edited by Grams/386.

RESULTS AND DISCUSSION

The S^{2}FT-IR PAS experimental results and data manipulations for the EVAc/PP sample collected at a phase modulation frequency of 200 Hz are illustrated in Figures 2−6 and summarized in Table 1. It should be noted that the thermal diffusivity values for EVAc and PP (1.34×10^{-3} and 0.78×10^{-3} cm^2/s, respectively) are close enough that the interfacial optical/thermal reflection effects can be reasonably ignored. Since most organic polymeric materials have a thermal diffusivity value of about 1.00×10^{-3} cm^2/s, assumption of this value as an average allows a valid and convenient PAS analysis for laminar polymers.

(Note: If thermal diffusivity values are significantly different for the two layers, then optical/thermal reflection effects cannot be ignored. This will complicate phase analysis,[19] since, in this case, much less light penetrates through the first layer and much weaker signals will originate from the second layer than in the thermally homogeneous case. Furthermore, the thermal wave reflection at the interface will affect the "true phase angle detection".)

Phase Rotation Method. Figure 2 shows the magnitude spectrum and the spectral components at two phase rotation angles of 80 and 115°. It can be seen from Figure 2 that the major EVAc bands A_1 (1740 cm^{-1}, C═O stretching), A_2 (1243 cm^{-1}, C—O stretching), and C_1 (2922 cm^{-1}, C—H stretching, overlapping band contributed mostly from the EVAc film) are enhanced at a phase rotation angle of 115°, while the PP bands, B (1169 cm^{-1}, C—C stretching) and the overlapping bands contributed mainly from

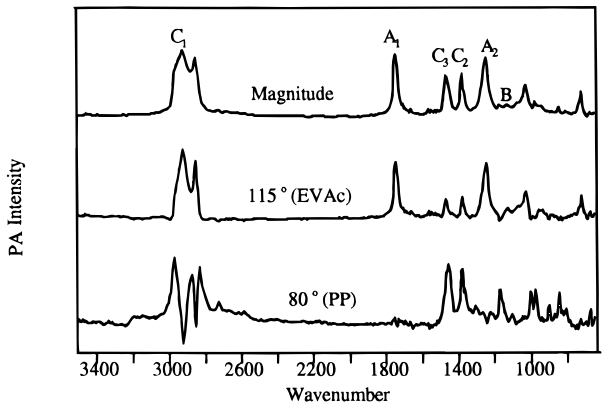

Figure 2. PA magnitude spectrum of EVAc (12 μm) on PP (60 μm) collected at a modulation frequency of 200 Hz; spectral components at 80 and 115°, respectively.

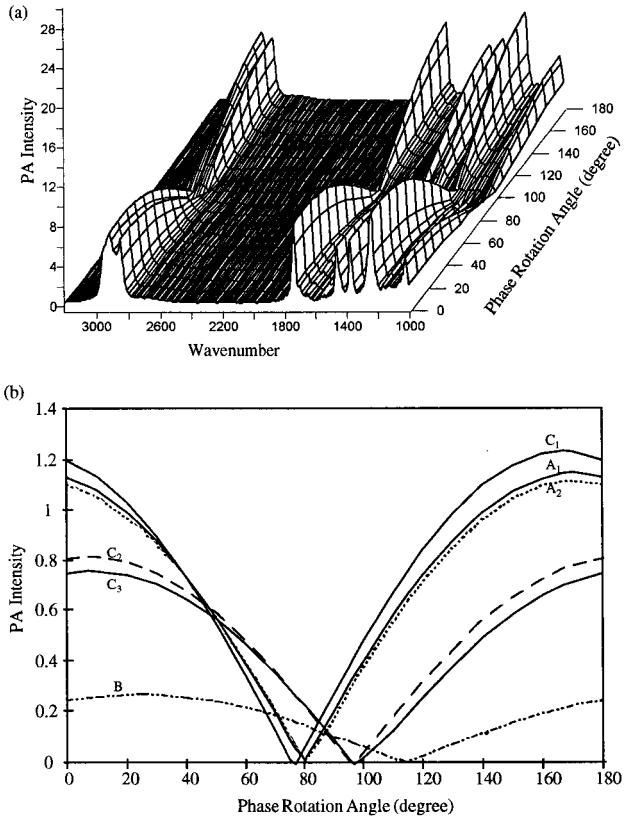

Figure 3. 3D (a) and 2D (b) representations of PA intensity variation of characteristic bands of EVAc (12 μm) on PP (60 μm) over the phase rotation range of 0−180°.

the PP, C_2 (1378 cm^{-1}, C—H bending) and C_3 (1463 cm^{-1}, C—H bending), are minimized at this angle. Exactly the reverse effect is observed at a phase rotation angle of 80°.[26]

The graphic illustration of the continuous phase rotation plot approach for the data in Figure 2 is shown with both three-dimensional (3D) and two-dimensional (2D) views in Figure 3a and b, respectively. It can be seen from Figure 3b that the PA intensity variation of characteristic bands of EVAc/PP over the phase rotation range from 0 to 180°. For example, pure EVAc bands A_1 and A_2 and the overlapping band C_1 are nulled first, and then the overlapping bands C_2 and C_3, while the nonoverlapping

(26) Independently measured spectra of the pure components show that the absorbance at 2922 cm^{-1} is relatively stronger in EVAc than in PP, while the opposite is true for absorption at 1378 and 1463 cm^{-1}.

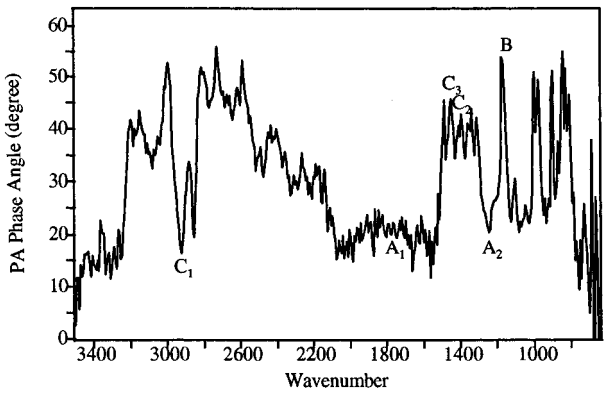

Figure 4. PA phase (relative) spectrum of EVAc/PP corresponding to the magnitude spectrum in Figure 2.

PP band B is nulled finally (at ~115°) within this phase rotation range. It can also be seen from the same figure that the difference in phase angle at which the intensities of the strongest surface band A_1 and the weakest substrate band B are nulled (or maximized) is ~35° (= 115°−80°). This is exactly the phase difference of the two phase-rotated spectra shown in Figure 2.

Phase Spectrum Method. Figure 4 is the corresponding relative phase spectrum of the EVAc/PP sample, which was calculated from the in-phase and quadrature spectra according to eq 1. As detailed in Table 1, bands A_1, A_2, and C_1 are associated with relatively smaller phase lags ranging from 16.5 to 20.4°, indicating shallower spatial origins of these signals, while bands C_2, C_3, and B exhibit relatively larger phase lags ranging from 36.4 to 53.3°, consistent with their deeper spatial origins. The difference between the phases associated with the strongest nonoverlapping absorption band of the EVAc layer (A_1) and the weakest nonoverlapping absorption band of the PP (B) is 32.9° (= 53.3° − 19.4°), which corresponds very closely to the 35° obtained by using the continuous phase rotation plot method.

Comparison between Phase Rotation and Phase Spectrum Methods. The PA phase differences between the strongest surface band C_1 and all other bands measured from the continuous phase rotation plot ($\Delta\theta_r$) and from the phase spectrum ($\Delta\theta_s$) are shown in Table 1 for comparison. It is clear that similar results have been obtained from both methods, as theoretically predicted. However, the phase spectrum method is generally more accurate, direct, and efficient than the phase rotation plot method. Although the phase rotation method has a certain visual appeal, it is much more computationally intensive since, in the phase spectrum method, only a single calculation is involved. While regions of the phase spectrum between bands [where $I(\sigma)$ and $Q(\sigma)$ both approach zero] naturally produce only noise, the result in regions of absorption is clear and quantitative.

2D Correlation Method. The synchronous and asynchronous 2D representations of the EVAc/PP PAS data obtained at a modulation frequency of 200 Hz are shown in Figures 5 and 6, respectively. It can be seen from the *synchronous* map that strong cross peaks (correlation contours related to two different peaks) appear at locations defined by the intersection of frequencies of any two of the four peaks: A_1 (C═O stretching), A_2 (C—O stretching), C_2 (C—H bending), and C_3 (C—H bending), such as A_1A_2,[27] A_1C_2, and A_1C_3, etc., which means that all four of these

(27) A_1A_2 is the short notation for cross peak $A_1(\sigma_1)A_2(\sigma_2)$, where σ_1 and σ_2 are wavenumbers on the *x*-axis and *z*-axis of the 2D map, respectively.

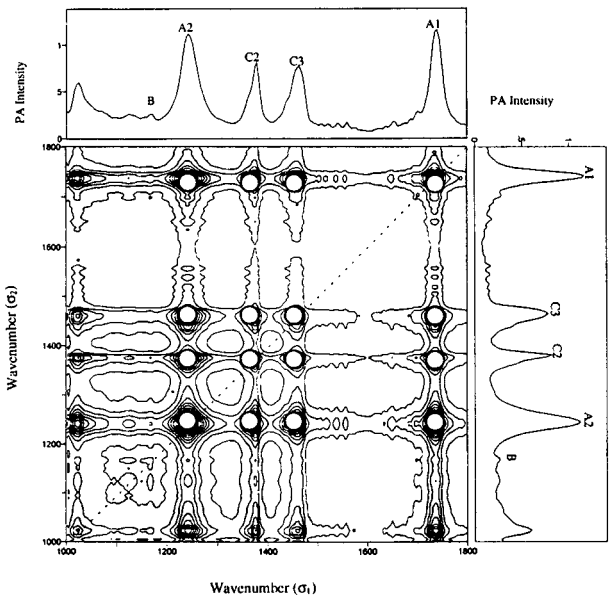

Figure 5. Synchronous 2D-IR representation of EVAc (12 μm) on PP (60 μm) PAS depth profiling data collected at a modulation frequency of 200 Hz. ○ = positive peak; ● = negative peak.

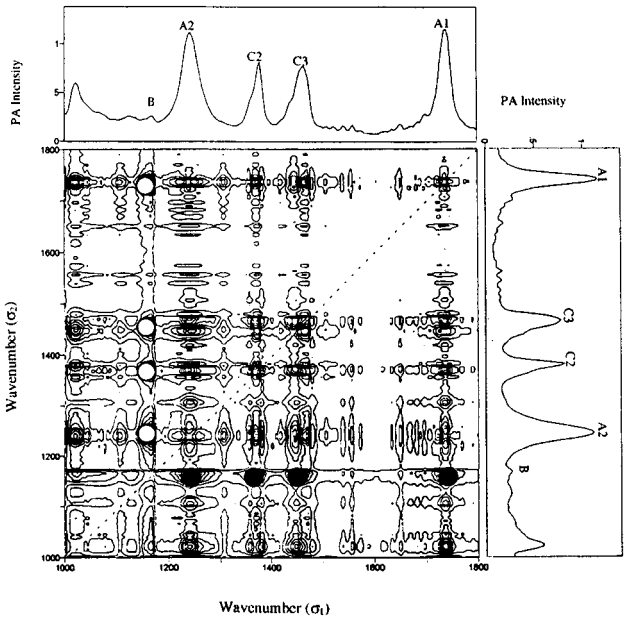

Figure 6. Asynchronous 2D-IR representation of EVAc (12 μm) on PP (60 μm) PAS depth profiling data collected at a modulation frequency of 200 Hz. ○ = positive peak; ● = negative peak.

peaks have similar signal phases, and thus their spatial origins (depths) are relatively close. However, cross peaks between peak B (C—C stretching) and any of the other four peaks are barely seen on the synchronous map, indicating that peak B has a very different signal phase from that of the others. This qualitative analysis is in accord with the results obtained from the phase spectrum method discussed above.

On the other hand, from the *asynchronous* correlation map (Figure 6), it can be seen that cross peaks generated from peak B and any of the other four peaks, A_1, A_2, C_2, and C_3, are considerably more intense than the other cross peaks, even though the magnitude of peak B itself is the weakest among them all. This, again, indicates a relatively large phase difference between peak B and the other four peaks. It can be further seen from the asynchronous map that cross peaks BA_1, BA_2, BC_2, and

BC_3 are all negative. This indicates that the detection of absorption band B occurs after that of all other bands A_1, A_2, and C_3, according to the rules originally proposed by Noda[24] for the analysis of 2D correlation maps. This conclusion, again, agrees with the results obtained from the phase spectrum method.

Limitations of 2D Correlation in Depth Profiling. Although we see from this example that there is general agreement between the 2D-PAS correlation analysis and the PA phase analysis (particularly the PA phase spectrum method), the limitations of the 2D approach to depth profiling studies are obvious. A 2D correlation map is a combined picture of both signal magnitude and phase; therefore, all the quantitative phase information is naturally hidden in the beauty of the 2D contours. While the 2D-PAS approach provides qualitative distinctions between spectral bands with quite different response phases, it cannot easily differentiate bands with close response phases, such as peaks A_1, A_2, C_1, and C_2 of the EVAc/PP sample. Furthermore, when the phase difference between two bands is neither nearly negligible (approaching zero) nor significantly out of phase (close to 90° difference), both the synchronous and asynchronous maps will show similar cross peaks. In the study of samples containing more than two layers, the 2D correlation method will encounter more difficulties, because bands of intermediate layers with phase differences close to 45° will show similar correlation on both synchronous and asynchronous spectra, and the order of the layers will usually be hard to determine from the 2D maps.

The significant advantage of 2D correlation analysis is its effective enhancement of spectral resolution, particularly in the asynchronous correlation. However, while new peaks are generated in the 2D correlation, which in some cases may reveal true spectral structure, in others, totally artificial (mathematical) creations without corresponding physical meanings may appear, and caution must be taken in analyzing these apparently high-resolution 2D peaks to avoid overinterpretation.

SUMMARY

In this paper, three PA phase-related analytical approaches used in S^2FT-IR PAS depth profiling have been demonstrated, compared, and evaluated for the analysis of a two-layered polymer sample, EVAc/PP. Similar/identical PA depth distinction can be obtained by using either the continuous phase rotation plot or the phase spectrum, as theoretically predicted. However, the phase spectrum method is generally more accurate, direct, and efficient than the phase rotation plot method. This advantage is quite obvious for depth profiling of ultrathin layered films or any quantitative depth profiling studies where high phase resolution is required. Although the continuous phase rotation plot method is more visually appealing in certain ways than the phase spectrum method, it is much more computationally intensive. This may result in time-consuming analysis if the relevant software package is not available.

Although qualitative agreement between the 2D correlation analysis and the PA phase analysis is observed, obvious limitations of the 2D approach to its further applications to depth profiling exist. A 2D-PAS correlation map is a combined picture of both PA signal magnitude and phase, and therefore the quantitative phase information is obscured. Furthermore, differentiation of correlation peaks with similar phases in multilayer samples can be ambiguous.

Received for review October 23, 1996. Accepted February 15, 1997.[⊗]

AC961080L

[⊗] Abstract published in *Advance ACS Abstracts,* April 1, 1997.